Coexistence of superparamagnetism and ferromagnetism in Co-doped ZnO nanocrystalline films

Qiang Li,[a] Yuyin Wang,[b] Lele Fan,[b] Jiandang Liu,[a] Wei Kong[a] and Bangjiao Ye[a,*]

[a]State Key Laboratory of Particle Detection and Electronics, University of Science and Technology of China, Hefei 230026, People's Republic of China
[b]National Synchrotron Radiation Laboratory, University of Science and Technology of China, Hefei 230029, People's Republic of China

Pure ZnO and $Zn_{0.95}Co_{0.05}O$ films were deposited on sapphire substrates by pulsed-laser deposition. We confirm that the magnetic behavior is intrinsic property of Co-doped ZnO nanocrystalline films. Oxygen vacancies play an important mediation role in Co–Co ferromagnetic coupling. The thermal irreversibility of field-cooling and zero field-cooling magnetizations reveals the presence of superparamagnetic behavior in our films, while no evidence of metallic Co clusters was detected. The origin of the observed superparamagnetism is discussed.
© 2013 Acta Materialia Inc. Published by Elsevier Ltd. All rights reserved.

Dilute magnetic semiconductors (DMSs) have attracted increasing attention in the past decade due to their promising technological applications in the field of spintronic devices [1]. Transition metal (TM)-doped ZnO is one of the most attractive DMS candidates because of its outstanding properties, including room-temperature ferromagnetism. However, the origin and mechanism of the observed ferromagnetism is far from being clearly understood, since experimental and theoretical studies on the magnetic properties of TM-doped ZnO show a number of contradictions. Although the ferromagnetic properties of Co-doped ZnO were observed in many reports [2–4], the paramagnetic and antiferromagnetic behaviors have also been demonstrated in $Zn_{1-x}Co_xO$ samples [5,6]. Several studies claim that the ferromagnetic properties arise from the formation of Co clusters or secondary phases; whereas others suggest that the Co clusters are correlated to the superparamagnetism and make no contribution to the observed ferromagnetism [7–9].

The magnetic properties of Co-doped ZnO remain a controversial topic. Detailed researches are required to provide experimental evidence of the mechanism of the magnetic properties in this system. In this work, the correlation between the structural features and magnetic properties of Co-doped ZnO films was clearly demonstrated.

The $Zn_{0.95}Co_{0.05}O$ films were deposited on sapphire (0 0 0 1) substrates by pulsed-laser deposition using a KrF excimer laser ($\lambda = 248$ nm) operating at 5 Hz and 200 mJ pulse^{-1}. The deposition was performed at 550 °C under oxygen partial pressures of 2×10^{-4} and 10 Pa. For comparison, a pure ZnO film was also prepared under identical growth conditions with an oxygen partial pressure of 2×10^{-4} Pa. The deposition time was 20 min and the thickness of the films detected by the stylus surface profiler was ~280 nm. The crystal structures and chemical valence states were characterized by 18 kW rotating anode X-ray diffraction (XRD) and X-ray photoelectron spectroscopy (XPS), respectively. Positron annihilation spectroscopy and Raman spectroscopy were used to investigate the defective condition in the films. For further insight into the structural properties, high-resolution transmission electron microscopy (HRTEM) and mapping analysis were also performed. Vibrating sample magnetometry (VSM) with an accuracy of 10^{-7} emu was used to determine the magnetic properties.

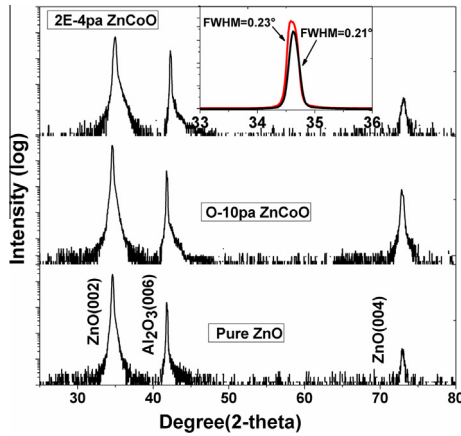* Corresponding author. Tel.: +86 0551 3607404; e-mail: bjye@ustc.edu.cn

Figure 1. The XRD patterns of $Zn_{0.95}Co_{0.05}O$ and pure ZnO thin films. Inset: ($0\,0\,2$) peak of pure ZnO and $Zn_{0.95}Co_{0.05}O$ prepared under an oxygen pressure of 10 pa.

The XRD patterns (Fig. 1) clearly show that only the ($0\,0\,2$) and ($0\,0\,4$) wurtzite hexagonal peaks of ZnO can be observed. No extra second-phase diffraction peaks corresponding to Co-related secondary phases or impurities are detected within the XRD detection limit, indicating that the Co-related clusters typically comprise no more than 1% within the ZnO lattices [10]. Also visible in the inset is the full width at half-maximum (FWHM) comparison of the ZnO ($0\,0\,2$) peak of pure ZnO and $Zn_{0.95}Co_{0.05}O$ film prepared under 10 Pa. A slight left broadening of the FWHM from 0.21° to 0.23° indicates that the Co-doped films are well crystallized with the Co^{2+} ions incorporated into the ZnO lattices.

The magnetic properties of pure ZnO and $Zn_{0.95}Co_{0.05}O$ films measured by VSM are displayed in Figure 2. The diamagnetic background of the substrate was subtracted from all the curves. Despite the identical growth conditions, pure ZnO film shows diamagnetic behavior at room temperature, while Co-doped ZnO films exhibit relative magnetization with S-shaped

curves, as shown in Figure 2a. This result confirms that intrinsic defects such as V_O, V_{Zn} or Zn_i do not introduce visible magnetic behavior in our samples, although defect-induced magnetism was demonstrated in previous studies [2]. Thus, the magnetization observed in Co-doped films is inevitably considered to be due to the presence of Co ions. The Co–ZnO film prepared under an oxygen pressure of 10 Pa showed a slight S-shaped M–H curve. However, no apparent coercive field (H_C) and discernible saturation magnetization (M_S) was observed. The M–T curves measured in field-cooling/zero field-cooling (FC/ZFC) under 500 Oe display analogous behavior and rapidly decrease with temperature from 5 to 50 K, and are then almost flat with temperature above 50 K, as shown in Figure 2c. This indicates that the dominant magnetic behavior in this sample is paramagnetism, and that a very weak ferromagnetism may coexist with this. For the $Zn_{0.95}Co_{0.05}O$ film prepared under 2×10^{-4} Pa, the ferromagnetism was clearly observed at room temperature and the magnetization is much larger than that of $Zn_{0.95}Co_{0.05}O$ film prepared under 10 Pa, which is in agreement with previous reports [11]. The H_C shown in the inset of Figure 2a is nearly zero (~20 Oe) at 300 K. However, the M–H curve measured at 5 K (Fig. 2b) displays a considerable hysteresis loop with the H_C value of 460 Oe, and the M_S increased from 0.72 to 1.51 μB per Co as the temperature decreased from 300 to 5 K. This implies that the film contains both ferromagnetic and paramagnetic behavior at room temperature. Figure 2d shows an irreversible FC/ZFC curve of M–T with T_{irr} ~30 K and the peak of M_{ZFC} at about 15 K, which is typical for superparamagnetic behavior arising from nanoscale grains. The increase of coercive field and saturation magnetization with the temperature from 300 K down to 5 K indicates a magnetic transition from superparamagnetism to ferromagnetism [12]. The transition temperature is dependent on the grain size. As shown in Figure 2d, the average value of the transition temperature in our film is about 15 K, which is in good agreement with the discrepancy between the magnetization loops measured at 5 and 300 K.

In order to reveal the mechanism of ferromagnetism and the cause of the magnetic difference between $Zn_{0.95}Co_{0.05}O$ films prepared at 10 and 2×10^{-4} Pa, as well as the origin of the observed superparamagnetism, a series of experimental analyses on the structure and defects of films were performed as shown in Figure 3.

As a sensitive tool for detecting negatively charged and neutral vacancy-type defects in materials, positron annihilation spectroscopy was employed to detect V_{Zn}-related defects in our films. The concentration of V_{Zn} was characterized by the Doppler broadening parameter, S, which is defined as the fraction of counts in the central area of the 511 keV annihilation peak [13]. The S parameters as a function of the incident positron energy for $Zn_{0.95}Co_{0.05}O$ films are shown in Figure 3a. Both the S–E curves show a slight change in slope at the film–substrate interface. This indicates that the film thickness is about 284 nm, which is in good agreement with the results of the stylus surface profilometry. Importantly, S-parameters in sample layers of the films did not show any difference, indicating an almost
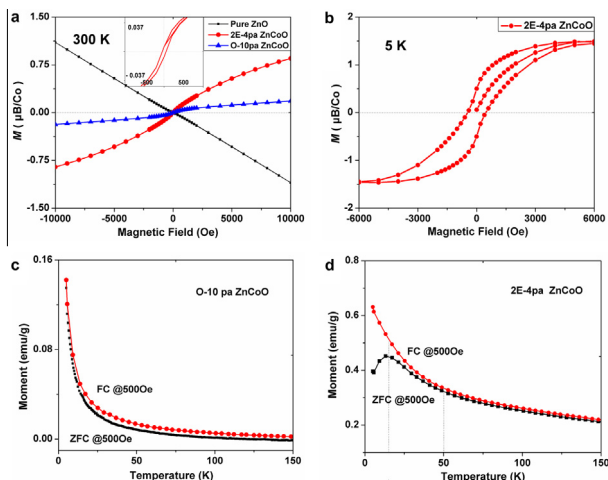

Figure 2. (a) Hysteresis loops measured at 300 K for pure and Co-doped ZnO films. (b) Hysteresis loops measured at 5 K for $Zn_{0.95}Co_{0.05}O$ film prepared under 2×10^{-4} Pa. Temperature-dependent magnetization measured in field-cooling and zero field-cooling (FC/ZFC) under 500 Oe for (c) $Zn_{0.95}Co_{0.05}O$ film prepared under 10 pa and (d) $Zn_{0.95}Co_{0.05}O$ film prepared under 2×10^{-4} Pa.
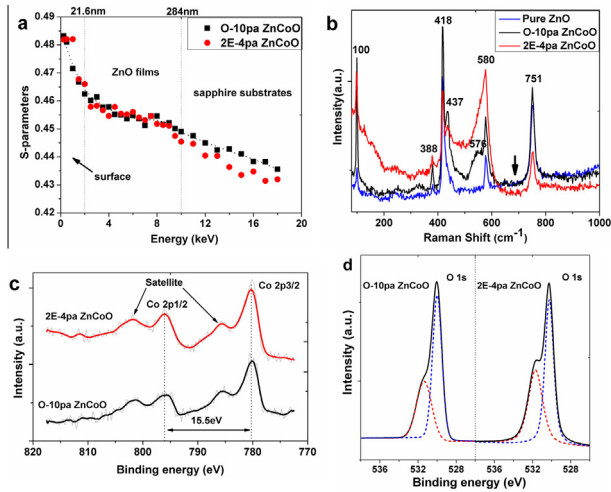
Figure 3. (a) The S-parameter as a function of positron implantation energy for Co-doped ZnO films. (b) Raman spectra of pure ZnO film and $Zn_{0.95}Co_{0.05}O$ films. XPS analysis of core levels for (c) Co $2p$ peaks, and (d) O $1s$ peaks in $Zn_{0.95}Co_{0.05}O$ films.

identical situation of V_{Zn}-related defects in the two films. Furthermore, V_{Zn}-related defects cannot be the origin of the difference in magnetism of the $Zn_{0.95}Co_{0.05}O$ films prepared at 10 and 2×10^{-4} Pa. The room-temperature Raman spectra were measured using a 514.5 nm excitation line from an Ar^+ ion laser, as shown in Figure 3b. Besides the phonon modes of the substrate (418 and 751 cm^{-1}), the expected ZnO modes located at 100 cm^{-1} = E_2 (low), 388 cm^{-1} = A_1 (TO), 437 cm^{-1} = E_2 (high), and 580 cm^{-1} = A_1 (LO) were also observed [14]. No $Zn_yCo_{3-y}O_4$-related impurity modes were detected by Raman spectroscopy, indicating a good solid solution of Co ions in the ZnO lattices. A relatively larger intensity of A_1 (LO) mode was observed in $Zn_{0.95}Co_{0.05}O$ film prepared under 2×10^{-4} Pa, which is due to the V_O-related complex defects [15]. Co $2p$ XPS spectra of $Zn_{0.95}Co_{0.05}O$ films are shown in Figure 3c. The binding energies of Co $2p_{3/2}$ are located at 780.2 eV and the energy gap between Co $2p3/2$ and $2p1/2$ is 15.5 eV, which corresponds to those reported for the core-level XPS spectrum of Co^{2+} ions in CoO, indicating a good substitution of high-spin Co^{2+} for the Zn^{2+} sites [16]. No impurities, such as metallic Co or Co_2O_3 clusters, were detected by XPS spectra. The average Co concentration was estimated to be 5.73 and 5.08 at.% for film prepared under 10 and 2×10^{-4} Pa, respectively. Although the presence of metallic Co clusters cannot be completely excluded by XRD and XPS analysis, the observed ferromagnetism in $Zn_{0.95}Co_{0.05}O$ films can be definitely attributed to the substitutional Co^{2+} instead of Co clusters. Otherwise, the measured moment of 1.51 μB per Co (for the film prepared at 2×10^{-4} Pa measured at 5 K) indicates that about 90% of the Co atoms should exist in the form of Co metal (1.7 μB per Co), which would be detectable by XRD and XPS [17]. The O $1s$ XPS spectra of films prepared under 10 and 2×10^{-4} Pa (solid black lines in Fig. 3d) show an asymmetric peak, which can be fitted by two Gaussian curves. The low binding energy peak (blue dashes) is located at 530 eV for intrinsic binding energy of O^{2+} in ZnO crystals, and the high binding

energy peak (red dashes) is located at 531.6 eV for V_O-related defects [18]. Figure 3d clearly shows that both the intensity and the relative area of the high binding energy peak in the 2×10^{-4} Pa prepared sample are more pronounced than that of film prepared under 10 Pa. This indicates that the film prepared at 2×10^{-4} Pa contains more oxygen vacancies, which is consistent with the Raman spectroscopy results. Given this difference in magnetization, these oxygen vacancies may play a significant role in governing Co–Co ferromagnetic coupling. It has been suggested that localized carriers initiated by V_O introduce hybrid orbitals overlapping with the d-orbitals of adjacent Co and establish a long-range ferromagnetic coupling [19]. Moreover, the film prepared at 2×10^{-4} Pa and annealed at 700 °C in air shows a rapid decrease of V_O concentration, and the corresponding ferromagnetism almost disappeared. This further confirms the close relation between ferromagnetic behavior and oxygen vacancies in $Zn_{0.95}Co_{0.05}O$ films.

The superparamagnetism observed in the films prepared at 2×10^{-4} Pa has not yet been explained, since no evidence of ferromagnetic nanoparticles was detected using the above techniques. In order to search carefully for possible Co clusters, we employed HRTEM and mapping analysis to obtain more insight into the microstructural characteristics and the distribution of Co in the film, as shown in Figure 4.

Figure 4a and b displays low-magnification HRTEM images for the $Zn_{0.95}Co_{0.05}O$ film prepared under 2×10^{-4} Pa. The images reveal that the film consists of numerous nanoscale grains with different sizes. It is clear from Figure 4b that the diameter of the grains ranges from 5 to 20 nm. A high-magnification cross-sectional HRTEM image is shown in Figure 4c, which shows that the nanoparticles are single crystalline without apparent lattice mismatch [20]. The interplanar distance is measured to be 0.26 nm, indicating a (0 0 2) preferential orientation [21]. The selected-area electron diffraction (SAED) pattern (Fig. 4a inset) confirms that the grains exhibit a hexagonal wurtzite structure. Moreover, based on the SAED pattern and a series of
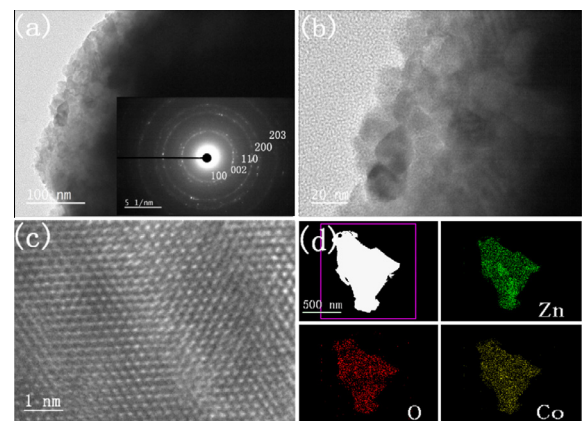

Figure 4. (a,b) Low-magnification HRTEM micrograph of $Zn_{0.95}Co_{0.05}O$ film prepared under 2×10^{-4} Pa. Inset of (a) is a selected-area electron diffraction (SAED) pattern of this film. (c) High-magnification cross-sectional HRTEM image. (d) Element mapping of Zn, O and Co for this film.

HRTEM image analyses, no evidence of Co metal clusters or other secondary phases was detected. These results are consistent with previous reports on Co-doped ZnO film at a doping concentration of 5 at.% [22,23]. Element mapping of Zn, O and Co (Fig. 4d) confirms that Co ions are randomly in solid solution in ZnO lattices and no sign of Co aggregation was observed, which is in good agreement with the XPS and Raman results. For Co-doped ZnO systems, although Co-cluster-induced superparamagnetism was demonstrated in previous research, we have not observed any trace of metallic Co clusters in our films by XRD, Raman, XPS, HRTEM and mapping analysis. An early report suggested that if the grain size of dilute magnetic nanofilms is small enough, some of the single-domain particles may interact with each other and exhibit superparamagnetic behavior [24]. It is worth noting that there are non-homogeneous distributions of oxygen vacancies in our film, as shown in Figure 4d. Those agglomerated oxygen vacancies can cluster the distribution of ferromagnetism, resulting in many superparamagnetic nanoclusters. This inference is consistent with the ferromagnetism in our film being an intrinsic property of nanocrystalline films, and not arising from Co-related clusters. It also explains the large changes in H_C and M_S when the temperature is reduced from 300 K down to 5 K.

In summary, we investigated the magnetic properties of $Zn_{0.95}Co_{0.05}O$ nanocrystalline films. The ferromagnetism observed in these films was attributed to the substitutional Co ions instead of Co cluster or Zn-related defects. Raman and XPS results indicate that the O vacancies play a role in governing Co–Co ferromagnetic coupling. For the film grown under a pressure of 2×10^{-4} Pa, the thermal irreversibility of FC/ZFC magnetizations definitely corresponds to the existence of superparamagnetism, which probably arises from the nanosize effect or non-homogeneous V_O-induced nanoscale aggregation of ferromagnetism.

[1] S.A. Wolf, D.D. Awschalom, R.A. Buhrman, J.M. Daughton, S. von Molnar, M.L. Roukes, A.Y. Chtchelkanova, D.M. Treger, Science 294 (2001) 1488.
[2] Neeraj Khare, Menno J. Kappers, Ming Wei, Mark G. Blamire, Judith L. MacManus-Driscoll, Adv. Mater. 18 (2006) 1449–1452.
[3] G. Ciatto, A. Di Trolio, E. Fonda, P. Alippi, A.M. Testa, A. Amore Bonapasta, Phys. Rev. Lett. 107 (2011) 127206.
[4] Q. Liu, C.L. Yuan, C.L. Gan, G.C. Han, J. Appl. Phys. 101 (2007) 073902.
[5] Tongfei Shi, Sanyuan Zhu, Zhihu Sun, Shiqiang Wei, Wenhan Liu, Appl. Phys. Lett. 90 (2007) 102108.
[6] P. Sati, C. Deparis, C. Morhain, S. Schafer, A. Stepanov, Phys. Rev. Lett. 98 (2007) 137204.
[7] Jung H. Park, Min G. Kim, Hyun M. Jang, Sangwoo Ryu, Young M. Kim, Appl. Phys. Lett. 84 (2004) 1338.
[8] T.C. Kaspar, T. Droubay, S.M. Heald, M.H. Engelhard, P. Nachimuthu, S.A. Chambers, Phys. Rev. B 77 (2008) 201303(R).
[9] He Wei, Tao Yao, Zhiyun Pan, Cong Mai, Zhihu Sun, Ziyu Wu, Fengchun Hu, Yong Jiang, Wensheng Yan, J. Appl. Phys. 105 (2009) 043903.
[10] Igor Djerdj, Georg Garnweitner, Denis Arcon, Matej Pregelj, Zvonko Jaglicic, Markus Niederberger, J. Mater. Chem. 18 (2008) 5208–5217.
[11] Q. Liu, C.L. Yuan, C.L. Gan, Guchang Han, J. Appl. Phys. 110 (2011) 033907.
[12] Rodrigue Lard, Etienne Talbot, Philippe Pareige, Herrade Bieber, Guy Schmerber, Silviu Colis, Veronique Pierron-Bohnes, Aziz Dinia, J. Am. Chem. Soc. 133 (2011) 1451–1458.
[13] J. Toivonen, T. Hakkarainen, M. Sopanen, H. Lipsanen, J. Oila, K. Saarinen, Appl. Phys. Lett. 82 (2003) 40.
[14] C. Sudakar, P. Kharel, G. Lawes, R. Suryanarayanan, R. Naik, V.M. Naik, J. Phys.: Condens. Matter. 19 (2007) 026212.
[15] J.S. Thakur, G.W. Auner, V.M. Naik, C. Sudakar, P. Kharel, G. Lawes, R. Suryanarayanan, R. Naik, J. Appl. Phys. 102 (2007) 093904.
[16] Hao Gu, Wen Zhang, Yongbing Xu, Mi Yan, Appl. Phys. Lett. 100 (2012) 202401.
[17] K.A. Griffin, A.B. Pakhomov, C.M. Wang, S.M. Heald, Kannan M. Krishnan, Phys. Rev. Lett. 94 (2005) 157204.
[18] M. Naeem, S.K. Hasanain, M. Kobayashi, Y. Ishida, A. Fujimori, Scott Buzby, S. Ismat Shah, Nanotechnology 17 (2006) 2675–2680.
[19] Nicola A. Spaldin, Phys. Rev. B 69 (2004) 125201.
[20] Debjani Karmakar, S.K. Mandal, R.M. Kadam, P.L. Paulose, A.K. Rajarajan, T.K. Nath, A.K. Das, I. Dasgupta, G.P. Das, Phys. Rev. B 75 (2007) 144404.
[21] Q. Liu, C.L. Yuan, C.L. Gan, Guchang Han, J. Appl. Phys. 110 (2011) 033907.
[22] R. Lardé, E. Talbot, F. Vurpillot, P. Pareige, G. Schmerber, E. Beaurepaire, A. Dinia, V. Pierron-Bohnes, J. Appl. Phys. 105 (2009) 126107.
[23] C. Song, K.W. Geng, F. Zeng, X.B. Wang, Y.X. Shen, F. Pan, Y.N. Xie, T. Liu, H.T. Zhou, Z. Fan, Phys. Rev. B 73 (2006) 024405.
[24] Haiyong Gao, M. Staruch, Menka Jain, Pu-Xian Gao, Paresh Shimpi, Paresh Shimpi, Yanbing Guo, Wenjie Cai, Hui-jan Lin, Appl. Phys. Lett. 98 (2011) 123105.